Electronic distributions in quasicrystalline Al-Pd-Mn alloys

1994 J. Phys.: Condens. Matter 6 8771

(http://iopscience.iop.org/0953-8984/6/42/009)

J. Phys.: Condens. Matter 6 (1994) 8771–8779. Printed in the UK

Electronic distributions in quasicrystalline Al–Pd–Mn alloys

Esther Belin†, Zoltán Dankházi†‡, Anne Sadoc§ and Jean Marie Dubois¶

† Laboratoire de Chimie Physique Matière et Rayonnement CNRS URA 176 and GDR CINQ, 11 rue Pierre et Marie Curie, 75231 Paris Cédex 05, France

‡ Institute for Solid State Physics, Muzéum krt 6-8, 1088 Budapest, Hungary

§ LURE, CNRS, MESR, CEA, and GDR CINQ, Université Paris-Sud, 91405 Orsay Cédex, France and LPMS, 49 avenue des Genettes, BP 9428, 95806 Cergy-Pontoise Cédex, France

¶ LSG2M CNRS URA 159 and GDR CINQ, Ecole des Mines, Parc de Saurupt, 54042 Nancy Cédex, France

Received 20 April 1994, in final form 27 July 1994

Abstract. We report on experimental valence and conduction electronic distributions of quasicrystalline Al–Mn–Pd alloys probed using the soft x-ray emission and absorption spectroscopy techniques. The various partial distributions are adjusted in the binding energy scale in order to investigate the electronic interactions characteristic in the material. In the valence band, interaction exists between Al states and Mn 3d states near the Fermi level and with Pd 4d states in the middle of the band. At the Fermi level the intensity of the Al 3p states is very low and a rather wide pseudo-gap is observed. In the conduction band, interaction exists also between Al p–Mn d states in the energy range of the absorption edge. Pd d–s states are found about 2 eV beyond the Fermi level. It is suggested that unlike the case of Mn, a small charge transfer may exist from Al to Pd states. Adjustment of Al 3p and Al p distributions at the same intensity at the Fermi level shows that the density of available Al p conduction states is dramatically decreased in the quasicrystal in comparison to pure Al. We propose that this could be connected to the existence of numerous narrow gaps and spikes in the densities of states as predicted theoretically elsewhere for crystal approximant phases with very large unit cells.

1. Introduction

In various stable quasicrystals of great structural quality such as Al–Cu–Fe, Al–Cu–Ru, Al–Pd–Re..., the densities of states (DOS) at the Fermi level (E_F) are rather low as compared to pure Al (Mori *et al* 1991, Belin *et al* 1992, Hippert *et al* 1992, Belin *et al* 1993, Stadnik and Stroink 1993) and unexpected high resistivities are found (see, for example Klein *et al* 1991, Basov *et al* 1994, Pierce *et al* 1993, Tamura *et al* 1994). For quasicrystalline Al–Pd–Mn alloys of high structural quality, it has been reported elsewhere that they also exhibit very high resistivity values at low temperatures (Lanco *et al* 1992, Akimaya *et al* 1993). Theoretical calculated densities of states that could provide insight into the electronic properties are available only for approximant crystalline phases of the quasicrystals (see, for example, Fujiwara and Yokokawa 1991, Fujiwara 1993, Fujiwara *et al* 1993, Krajci *et al* 1993). On the other hand, from measurements of valence band (VB) and conduction band (CB) electronic distributions, information on the actual electronic structure of a material may be obtained (see, for example, Belin *et al* 1992). Such information can be very helpful for the understanding of the physical and electronic properties of the quasicrystalline phases (Belin and Mayou 1993). We report here on an experimental investigation of valence and conduction states of single-phase quasicrystalline $Al_{71}Pd_{19}Mn_{10}$ and $Al_{70}Pd_{21}Mn_9$ alloys. The paper consists of two sections; in the first, we describe the experimental techniques

0953-8984/94/428771+09$19.50

which we have used for the measurements and in the second section we present and discuss the results.

2. Experimental procedure

The investigation of both VB and CB electronic distributions has been performed using the soft x-ray spectroscopy (SXS) technique. It is well known that x-ray transitions are governed by dipole selection rules and are transition probabilities dependent. Thus a main advantage of this technique is that it probes *separately* the valence and conduction electronic distributions for a given s, p, ... character around *each atomic site* in a solid whether it is metallic or not, crystalline, amorphous...

The valence partial DOSs were carried out using the x-ray emission (SXES) spectroscopy technique. Indeed, during the x-ray emission process, photons are emitted due to the radiative recombination of a core hole from the valence band; the emitted intensity is proportional to $\mathcal{N}_{\mathcal{E}\mathrm{occ}} * \mathcal{L}_{n,l}$ where $\mathcal{N}_{\mathcal{E}\mathrm{occ}}$ is the valence band DOS and $\mathcal{L}_{n,l}$ is the width of the inner level that is involved in the transition. The conduction partial DOSs were obtained using either photoabsorption (SXAS) or photoyield techniques. In SXAS, the intensity of an incident radiation is measured before (I_0) and after going though (I) the sample of suitable thickness; the photoabsorption coefficient μ, proportional to $\mathcal{N}_{\mathcal{E}\mathrm{unocc}} * \mathcal{L}_{n,l}$ ($\mathcal{N}_{\mathcal{E}\mathrm{unocc}}$ is the conduction band DOS and $\mathcal{L}_{n,l}$ has the same significance as above) is obtained owing to $\mu \sim \log I_0/I$ versus the energy of the incident photons. In the photoyield technique, a chosen inner electron of the solid is promoted to the conduction band by the energy of incoming photons; many electrons are emitted during the process, the number of which is connected to $\mathcal{N}_{\mathcal{E}\mathrm{unocc}} * \mathcal{N}_{n,l}$. The emitted electrons are collected by means of appropriate channeltrons and the intensity is measured against the variation of the incident photons' energy. The DOSs are proportional to the ratio I/I_0 where I_0 and I are the intensities of the incident photons and of the collected electrons respectively. Actually, $\mathcal{N}_{\mathcal{E}\mathrm{unocc}}$ is the conduction band DOS in the presence of a K or L inner hole. In some cases the presence of the inner hole induces significant perturbation of the conduction states that is seen as satellite lines whose intensities may sometimes be rather high. This is usually the case when strongly localized states are detected, for example 4f states in rare earths, but no such important modifications near the Fermi level are expected as far as extended states are investigated. As a matter of fact, the effect of the core hole on the DOS is not easily calculable. Van Acker *et al* (1991) have studied its eventual effect in comparing Ni L_{III} x-ray absorption edges of pure Ni, Ni_3B and NiB with calculated distribution of unoccupied d states in the ground state. They concluded that no effect of core hole was detected in these x-ray absorption spectra. Due to similarities between Ni and Mn or Pd, one expects the same could be true for the latter elements. Moreover, in quasicrystals the DOS at the Fermi level, although low, is not zero and important hybridization effects are seen. Therefore, possible screening effects due to the core hole could be averaged over the different partial DOS and could thus be negligible. Note also that recently calculations of partial DOS in Al_7Cu_2Fe, a crystalline phase of composition close to that of the perfect icosahedral quasicrystalline $Al_{62}Cu_{25.5}Fe_{12.5}$ alloy, performed without any core hole effect, were found to simulate quite well the experimental SXAS spectra (Trambly de Laissardière *et al* 1994). Consequently, our measurements provide a relevant picture of the conduction DOSs of the quasicrystalline materials.

The SXES and SXAS curves are normalized between their maximum intensity and ranges where the variation of intensity is negligible. Thus, no information can be deduced

concerning absolute DOSs. However, it makes sense to compare the shapes and intensities of different curves of a given spectral character in various materials, for example, the curves for Al in the pure metal and in the alloys.

The binding energies of inner levels of a solid may be obtained using the photoemission spectroscopy technique (XPS). This measures the kinetic energy of electrons of a solid once ejected by incident photons of appropriate energy. The binding energies are directly connected to the kinetic energies that are obtained with respect to the Fermi level of the solid, owing to convenient calibration of the energy scale (for example, by referring to the Au $4f_{7/2}$ level or contamination C 1s level binding energies). Thus, if one measures the binding energies of the inner levels involved in given x-ray transitions, it becomes feasible to locate the Fermi energy on the corresponding x-ray transition energy scales. Consequently, it is possible to adjust various partial DOSs as obtained by the SXS techniques to the same absolute binding energy scale with E_F taken as the origin.

To describe as totally as possible both valence and conduction bands, different partial DOSs have been probed as indicated in table 1. Let us recall that for Mn and Pd, the valence band spectra concern mainly the d states distributions. Indeed, the transition probabilities favour p–d transitions with respect to p–s ones and moreover s states are not dominant in the valence band.

Table 1. Name of transitions, probed electronic distributions, corresponding used experimental technique and experimented energy range. SXES: soft x-ray emission spectroscopy. SXAS: soft x-ray photoabsorption spectroscopy. Yield: photoyield spectroscopy.

Name of transition	Transition	Probed states	Experimental technique	Experimental energy range
Al Kβ	VB $\rightarrow$ 1s	3p	SXES	1545–1575 eV
Al $L_{2,3}$	VB $\rightarrow$ $2p_{3/2}$	3s–d	SXES	60–78 eV
Al K$\alpha_{1,2}$	$2p_{3/2} \rightarrow$ 1s	Atomic line	SXES	1485–1488 eV
Al K	1s $\rightarrow$ CB	p	Yield	1560–1590 eV
Pd L$\beta_{2,15}$	VB $\rightarrow$ $2p_{3/2}$	4d–s	SXES	3160–3185 eV
Pd L_{III}	$2p_{3/2} \rightarrow$ CB	d–s	Yield	3150–3250 eV
Pd K	1s $\rightarrow$ CB	p	SXAS	24 250–25 500 eV
Mn Lα	VB $\rightarrow$ $2p_{3/2}$	3d–s	SXES	630–637 eV
Mn L_{III}	$2p_{3/2} \rightarrow$ CB	d–s	Yield	635–650 eV
Mn K	1s $\rightarrow$ CB	p	SXAS	6500–6600 eV

The valence partial DOSs measurements were carried out with vacuum spectrometers fitted with bent $SiO_2(10\bar{1}0)$ or KAP crystals or a grating; the energy resolutions in the investigated energy ranges are ± 0.3 eV for both sets of equipment. The spectra were excited with either incoming electrons or photons on the samples that were water cooled and the emitted photons were collected in gas flow proportional counters. The conduction partial DOSs were obtained at the synchrotron facility of LURE. Measurements of the Pd K, Mn K and Pd L_{III} absorption edges involve the DCI radiation and SXAS technique. The yield technique was applied at the Super ACO storage ring for Al K and Mn L_{III} absorption edges. For probing Al p and Pd d–s states, we used two-crystal monochromators equipped with $SiO_2(10\bar{1}0)$ or Si(111) slabs, respectively, whose energy resolutions were about ± 0.3 eV. For investigating the Mn d–s states, a TGM monochromator was utilized, the resolution of which is about ± 0.2 eV in the experimental energy range (Tourillon 1992). Pd p and Mn p states were probed with a Si 311 channel cut single crystal to monochromatize the incident beam and ionization chambers filled with argon for Pd p edge and a mixing of helium and neon for the Mn p edge.

In all the experiments, pure Al, Pd and Mn were also measured for calibration purposes.

From XPS measurements we have obtained the Al $2p_{3/2}$, Mn $2p_{3/2}$ and Pd $3d_{5/2}$ binding energies with respect to the C 1s level taken equal to 285.0 eV. For Al, since the binding energy of the 1s level could not be obtained directly, we measured the $2p3/2 \rightarrow 1s$ emission line (Al Kα) and deduce the value for Al 1s. In the case of Pd, we did not measure directly the inner level involved in the probed x-ray transitions because its photoemission cross-section is rather low. We made the assumption that in the alloys with respect to the pure metal, the chemical shift is the same whatever the inner level may be. Then, we measured the Pd $2p_{3/2}$ binding energy whose photoemission cross section is higher than that of Pd $3d_{5/2}$. Thus, we locate E_F on the transition energy scales within ± 0.1 eV accuracy for Al and not better than ± 0.3–0.5 eV for the other elements.

Samples of nominal compositions as indicated in this paper were prepared by conventional solidification techniques. Details on the preparations conditions may be found, for example, in Beeli *et al* (1991). Structural data were supplied by combining various techniques namely electron microscopy (Dong *et al* 1991), x-ray and neutron diffraction (Boudard *et al* 1991, 1992) and EXAFS (Sadoc and Dubois 1992).

3. Results and discussion

We display in figure 1 the partial VB contributions of $Al_{71}Pd_{19}Mn_{10}$. Adjustment of these contributions accounts for the shift of the inner levels in the alloy with respect to the pure metals i.e. 0.5 ± 0.1 eV for Al $2p_{3/2}$, 0.2 ± 0.3–5 eV for Mn $2p_{3/2}$ and 1.5 ± 0.3–5 eV for Pd $3d_{3/2}$. This figure shows that: (i) near E_F, the maximum of the Mn 3d states distribution curve is superposed to the edge and shoulder of the Al 3p distribution, this latter is due to a bending of the curve just at the edge; (ii) at about $E_F + 3.5 \pm 0.3$ eV, Pd 4d states are present, (iii) Al 3p and 3s–d states distribution curves are separated into two parts located roughly on each side of the Pd 4d curve. They are superposed and extend over about 10 eV. Within the experimental uncertainties, the curves for the other samples of compositions $Al_{70}Pd_{21}Mn_9$ and also $Al_{71}Pd_{19}Mn_{10}$ are comparable, they are not shown here.

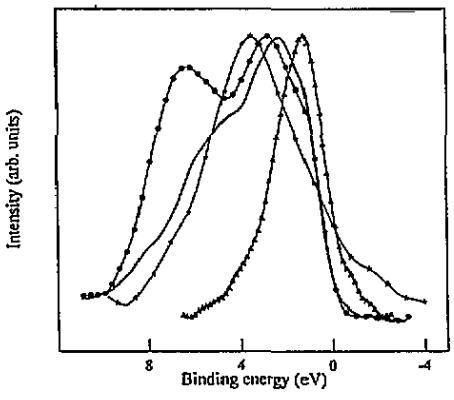

Figure 1. Partial valence band electronic distributions in quasicrystalline $Al_{71}Pd_{19}Mn_{10}$. Line with triangles: Mn 3d; full line: Al 3p; line with stars: Pd 4d; line with full circles: Al 3s-d.

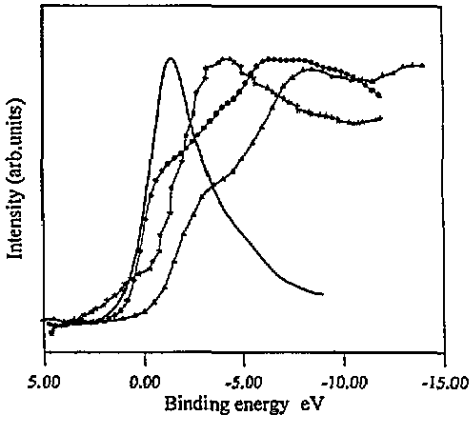

Figure 2. Partial conduction band electronic distributions in quasicrystalline $Al_{71}Pd_{19}Mn_{10}$. Full line: Mn d-s; line with full circles: Al p; line with stars: Pd d-s; line with triangles: Mn p.

The partial Pd and Mn VB DOSs retain the same shape in the respective metals and in the quasicrystal in contrast to the case of Al. As an example, let us consider the Al 3p distribution curve. The shape in pure Al is parabolic-like as is expected for a free-electron-like metal. This is no longer observed in the quasicrystalline alloy due to the splitting present in the middle of the sub-band; this gives indication that the free-electron model is no longer valid for the description of the electronic properties of the Al–Pd–Mn quasicrystals. On the other hand, because of the splitting of the distribution curves, the full width at half maximum (FWHM) intensity in the quasicrystals is larger than in the pure metal by about 0.5 eV. The maximum of the Pd 4d distribution in the alloys is shifted deep into the valence band by about 1.7 ± 0.3 eV from E_F with respect to pure Pd. According to the experimental accuracy, the FWHM is not significantly changed. Within the precision of the measurements, the maximum of the Mn 3d distribution in the quasicrystalline alloy is not shifted with respect to Mn, however, the FWHM is reduced to 2.5 ± 0.1 eV in the alloys against 3.5 ± 0.1 eV in the pure metal.

These modifications result from the various electronic interactions that exist between the different elements in the alloys as compared to the pure metals where all neighbour atoms are of the same kind. The interactions mainly take place via Mn 3d and Al states near E_F and between Pd 4d and Al states in the middle of the valence band.

Due to the interaction between Al and Mn d states in the close vicinity of E_F, the edge of the Al sub-bands is somewhat shifted towards increasing binding energies with respect to pure Al and very important is the reduction of the Al DOS at E_F: the intensity at E_F is 50% of the maximum intensity in pure Al whereas it is only 19% in the alloy. In pure Al, the valence band edge crosses E_F at its half intensity; in the icosahedral Al–Pd–Mn quasicrystals, the point to which the half maximum intensity corresponds is distant by $\delta = +0.7 \pm 0.1$ eV from E_F. The reduced Al density of states at E_F together with the backward shift of the Al valence band edge characterize a wide and deep pseudo-gap in the Al–Pd–Mn quasicrystals. Such a pseudo-gap is consistent with the fact that these quasicrystalline alloys are stabilized according to a Hume-Rothery mechanism (Hume-Rothery and Coles 1954, Friedel and Dénoyer 1987); as a result of this stabilization mechanism, electronic states are transferred from the vicinity of E_F to higher binding energies towards the centre of the valence band. From this point of view, Al–Pd–Mn quasicrystalline alloys can be compared to good quasicrystalline $Al_{63}Cu_{25}Fe_{12}$, where the pseudo-gap is characterized by the Al intensity at E_F of about 10% the maximum intensity and the distance $\delta = +0.6 \pm 0.1$ eV. Note that those quasicrystals have similar electronic properties. We shall come back later to this point.

The depletion of the Al curves in the middle of the valence band is a consequence of the interaction between Al states and Pd 4d states. This splitting is less marked in the Al 3p than in the Al 3s–d curve, however, in this latter case, in the energy range $E_F + 5$–$E_F + 9$ eV, it cannot be ruled out that an extra contribution due to oxide in the sample might affect the shape of the curve. So, in the following, we will no longer discuss the Al 3s–d distribution. Measurements will be undertaken in the near future in conditions such that no oxide contamination can remain in the sample.

We have plotted in figure 2 the Mn d–s, Pd d–s, Mn p and Al p distribution curves of the conduction band. From E_F to about $E_F - 1$ eV Mn d–s and Al p states distribution curves overlap. This indicates that Mn d–s and Al p states interact over all this energy range. At about $E_F - 5$ eV, the maximum of the Pd d–s curve coincides with a shoulder of both the Al p and Mn p DOS curves, consequently, Pd, Mn and Al states interact with each other in this energy range. Beyond this, towards decreasing energies from E_F, there are mainly Mn p and Al p states.

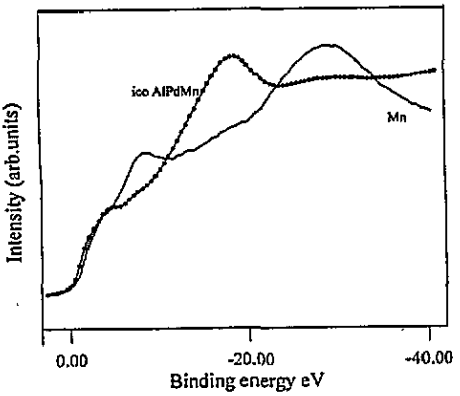

Figure 3. Mn p conduction band distributions in pure metallic Mn (full line) and in quasicrystalline $Al_{71}Pd_{19}Mn_{10}$ (line with full circles).

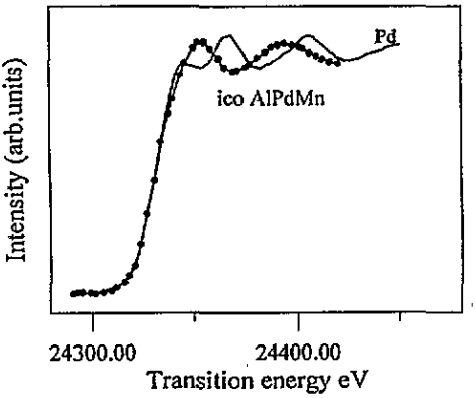

Figure 4. Pd p conduction band distributions in pure metallic Pd (full line) and in quasicrystalline $Al_{71}Pd_{19}Mn_{10}$ (line with full circles).

The Mn p and Pd p conduction electronic distributions in the quasicrystalline alloy and the pure metals are displayed in figures 3 and 4 respectively. The curves are shown in the x-ray transition energy scale for Pd. This is because in this case, we could not locate with enough accuracy the Fermi level energy on the x-ray transition energy scale for the alloy. These curves are quite different in metals and alloys particularly as far as the energy positions of the peaks are concerned. This stresses once more that hybridizations of Mn and Pd are modified in the alloys in comparison to the corresponding pure metals mostly due to the interactions with Al and because of the lack of same close neighbour atoms.

The Mn and Pd conduction d–s curves of the pure metals exhibit a prominent peak near E_F, the so called 'white line' which is d-like in character. This sharp shape is preserved for Mn d–s DOS of the quasicrystal but not for the Pd d–s DOS curve. Figure 5 shows that the Pd d–s curve for the quasicrystal is noticeably less sharp and is wider than in pure Pd. Again, this may be ascribed to a small charge transfer from Al to Pd states: this emphasizes strong modifications of Pd hybridizations due to the various electronic interactions in the alloy. This also points out that in quasicrystalline Al–Pd–Mn alloys, Pd d states should be more filled than in the pure metal whereas for Mn, there should remain almost as many empty d states as in the pure metal. This is unlike in the case of $Al_{62}Cu_{25.5}Fe_{12.5}$ quasicrystals where a notable charge transfer from Al to Fe d states located near E_F is observed. Our present result is surprising since the electronic properties of Al–Pd–Mn and Al–Cu–Fe quasicrystals are rather similar, in particular, both quasicrystals display resistivities of the same order of magnitude: about 10 000 $\mu\Omega$ cm (Berger *et al* 1993 and references therein). However, it is noteworthy that the local order is somewhat different in both materials: Fe atoms in icosahedral Al–Cu–Fe quasicrystal are surrounded by two shells of Al atoms whereas there is only one Al atoms shell around the Mn atoms in icosahedral quasicrystalline Al–Pd–Mn (Sadoc and Dubois 1992, Sadoc *et al* 1993).

We show in figure 6 the valence Al 3p electronic distribution curves that are adjusted to the Al 3p intensity value of E_F. Also, for comparison, we have plotted the same curves for pure Al. This figure points out the low Al DOS at E_F, the repulsion of the valence band edge towards the centre of the valence band and the dramatic depletion of the conduction states. This result is the same as for quasicrystalline $Al_{62}Cu_{25.5}Fe_{12.5}$ in particular over the energy range E_F to $E_F - 6$ eV (figure 7), it is consistent with the reduced conductivity of

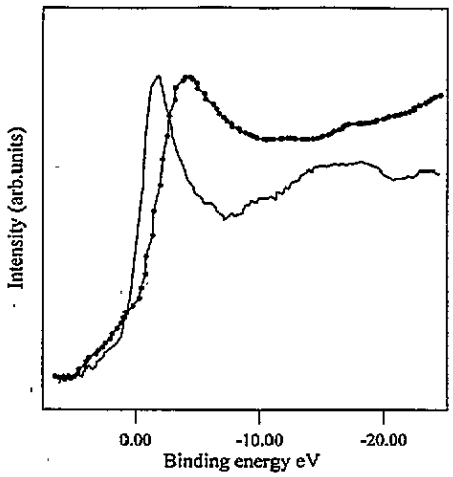

Figure 5. Pd d–s conduction band distributions in pure metallic Pd (full line) and in quasicrystalline $Al_{71}Pd_{19}Mn_{10}$ (line with full circles).

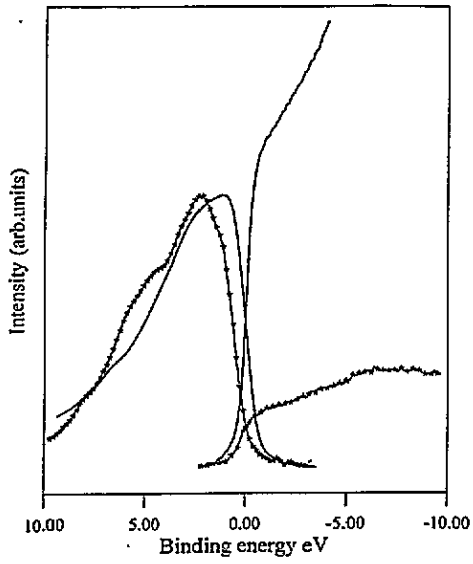

Figure 6. Valence band Al 3p and conduction band Al p distributions in pure Al (full line) and in quasicrystalline $Al_{71}Pd_{19}Mn_{10}$ (line with stars). At the Fermi level, the intensity of the Al p curves is adjusted to the value of the corresponding Al 3 p curve.

the Al–Pd–Mn quasicrystalline alloy since it shows that transitions to normally unoccupied states are rather improbable.

Our experimental result are consistent with the picture of quasicrystals as 'quantum-well-like' materials proposed recently by Janot and de Boissieu: for these authors, most of the electronic states are lying in the valence band whereas the conduction band is found to be rather depleted (Janot and de Boissieu 1994). On the other hand, DOS calculations for approximate phases have pointed out the existence of numerous narrow spikes and gaps (Fujiwara and Yokokawa 1991, Fujiwara 1993). In our experiments, as already indicated above, the density of conduction states is measured via transitions from an inner level to empty states, so that the unoccupied DOSs $\mathcal{N}_{\mathcal{E}\mathrm{unocc}}$ are convoluted by the energy distribution $\mathcal{L}_{n,l}$ of the inner level involved in the x-ray transition. Because the width of $\mathcal{L}_{n,l}$ is much wider than that of the spikes and gaps, the intensity which is observed experimentally is smoothed out and reduced to an average value with respect to the true intensity of the spikes and the deepness of the gaps. As a consequence, a low-density averaged continuous-like curve is obtained instead of a 'saw-like line' due to the succession of narrow gaps and spikes. Because of similarities we have observed experimentally between quasicrystals and their approximant phases, we may expect that the same features should exist in the DOS of approximants and real quasicrystals. As a matter of fact, we observe very low intensities in the Al p conduction spectra of both Al–Pd–Mn and Al–Cu–Fe quasicrystals. So, as already proposed for the $Al_{62}Cu_{25.5}Fe_{12.5}$ quasicrystal (Belin *et al* 1994) we suggest that the conduction Al p densities of states in the Al–Pd–Mn quasicrystals should also consist of a succession of narrow intense spikes and deep gaps leading to the low intensities of conduction Al p states observed experimentally beyond the Fermi level over a wide extent.

For $Al_{62}Cu_{25.5}Fe_{12.5}$ we have suggested that the high-resistivity values are connected to the importance of the pseudo-gap at the Fermi level and to the low intensity of Al p states

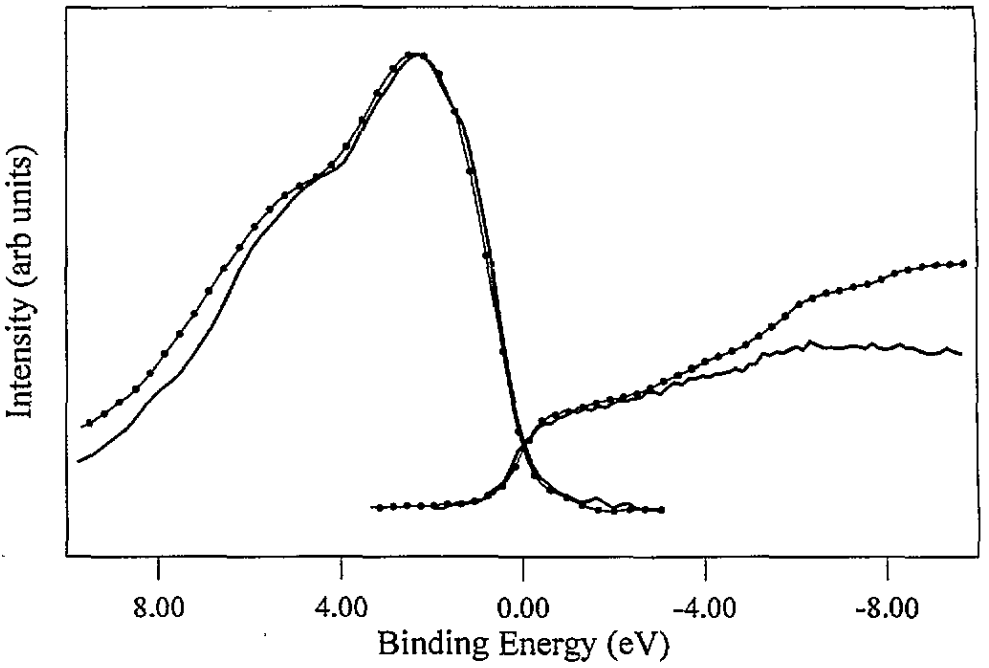

Figure 7. Valence band Al 3p (left side) and conduction band Al p (right side) distributions in quasicrystalline $Al_{62}Cu_{25.5}Fe_{12.5}$ (thin line with full circles) and in quasicrystalline $Al_{71}Pd_{19}Mn_{10}$ (thick line), both sets of curves are adjusted in the intensity scale to the Al 3p curve value at the Fermi level.

distribution over a wide energy range apart from E_F (Belin *et al* 1994). The same should be true for Al–Pd–Mn quasicrystals. However, note that recently (Fujiwara *et al* 1993, Fujiwara and Trambly de Laissardière 1994) emphasized that for approximant structures of quasicrystalline alloys, not only the pseudo-gap at E_F but also the numerous deep narrow gaps of the DOS should play an important role in the electronic properties of the approximants especially the high resistivity and the optical conductivity. The same should hold true for the related quasicrystals since, as mentioned above, we observe similarities in our experimental results between approximant and quasicrystalline alloys.

To summarize, our investigation of the valence and conduction electronic distributions in Al–Pd–Mn quasicrystals has revealed that Al and Mn states, in strong interaction, are present near the Fermi level whereas Pd states are found at about 4 eV from each side of E_F. A slight charge transfer to Pd from Al states is shown. We have observed a drastic depletion of Al states from each side of E_F that leads to the low Al DOS as E_F, to the repulsion towards the centre of the valence band of the Al 3p edge as well as to the reduced intensity of the conduction Al p band. These results are similar to those reported elsewhere for Al–Cu–Fe approximants and quasicrystals. By analogy, we ascribe the strong depletion of the Al p conduction band of quasicrystalline Al–Pd–Mn alloy to a succession of numerous narrow gaps and spikes in the DOS.

Acknowledgments

Drs J-B, Suck and C Beeli are warmly thanked for kindly supplying their $Al_{71}Pd_{19}Mn_{10}$

and $Al_{70}Pd_{21}Mn_9$ samples. It is also a pleasure to thank A M Flank, I Ascone, S Benazeth, R Cortès, P Lagarde and G Tourillon for invaluable assistance during the experiments at LURE. EB is indebted to Professors C Bonnelle and J F Sadoc and to Drs P Garoche and D Mayou for interesting discussions. ZD acknowledges financial support from grants TEMPUS no HUS-017–91 and BGF no 92–108.

References

Akiyama H, Hashimoto T, Shibuya T, Edagawa K and Takeuchi S 1993 *J. Phys. Soc. Japan* **62** 639
Basov D N, Pierce F S, Volkov P, Poon S J and Timusk T 1994 *Phys. Rev. Lett.* submitted
Beeli C, Nissen H U and Robadey J 1991 *Phil. Mag. Lett.* **63** 87
Belin E, Dankhazi Z and Sadoc A 1993 *J. Non-Cryst. Solids* **156–158** 896
Belin E, Dankhazi Z, Sadoc A, Calvayrac Y and Dubois J M 1994 *Europhys. Lett.* **26** 677
Belin E, Dankhazi Z, Sadoc A, Calvayrac Y, Klein T and Dubois J M 1992 *J. Phys.: Condens. Matter* **4** 4459
Belin E and Mayou D 1993 *Phys. Scr.* **49** 356
Berger C, Belin E and Mayou D 1993 *Ann. Chim. Fr.* **18** 485
Boudard M, de Boissieu M, Janot C, Dubois J M and Dong C 1991 *Phil. Mag. Lett.* **64** 197
Dong C, Dubois J M, de Boissieu M, Boudard M and Janot C 1991 *J. Mater. Res.* **6** 1
Friedel J and Dénoyer F 1987 *C. R. Acad. Sci.* II **305** 171
Fujiwara T 1993 *J. Non-Cryst. Solids* **153–154** 390
Fujiwara T and Trambly de Laissardière G 1994 *Mater. Sci. Eng.* at press
Fujiwara T, Yamamoto S and Trambly de Laissardière G 1993 *Phys. Rev. Lett.* **71** 4166
Fujiwara T and Yokokawa T 1991 *Phys. Rev. Lett.* **63** 333
Hippert F, Kandel L, Calvayrac Y and Dubost B 1992 *Phys. Rev. Lett.* **69** 2086
Hume-Rothery W and Coles B R 1954 *Adv. Phys.* **3** 149
Ibberson R, Audier M and Dubois J M 1992 *J. Phys.: Condens. Matter* **4** 10 149
Janot C and de Boissieu M 1994 *Phys. Rev. Lett.* **72** 1674
Klein T, Berger C, Mayou D and Cyrot-Lackmann F 1991 *Phys. Rev. Lett.* **66** 2907
Krajci M and Hafner J 1993 *J. Non-Cryst. Solid.* **156–158** 887
Lanco P, Klein T, Berger C, Cyrot-Lackmann F, Fourcaudot G and Sulpice A 1992 *Europhys. Lett.* **18** 227
Mori M, Matsuo S, Ishimasa T, Matsuura T, Kamiya K, Inokuchi H and Matsukawa T 1991 *J. Phys.: Condens. Matter* **3** 767
Pierce F S, Poon S J and Guo Q 1993 *Science* **261** 737
Sadoc A, Berger C and Calvayrac Y 1993 *Phil. Mag.* B **68** 475
Sadoc A and Dubois J M 1992 *Phil. Mag.* B **66** 541
Stadnik Z M and Stroink G 1993 *Phys. Rev.* B **47** 100
Tamura R, Waseda A, Kimura K and Ino H 1994 *Mater. Sci. Eng.* at press
Trambly de Laissardière G, Dankhazi Z, Belin E, Sadoc A, Nguyen Manh D, Mayou D, Keegan M A and Papaconstantopoulos D A 1994 *Phys. Rev.* B submitted
Tourillon G 1992 *Rapport d'Activité* LURE, ligne SACEMOR
Van Acker J F, Lineyer E W and Fuggle J C 1991 *J. Phys.: Condens. Matter* **3** 9579